International Journal for Computational Methods in Engineering Science and Mechanics

ISSN: 1550-2287 (Print) 1550-2295 (Online) Journal homepage: www.tandfonline.com/journals/ucme20

Natural Convection Heat and Mass Transfer in a Micropolar Fluid with Thermal and Mass Stratification

D. Srinivasacharya & C. Ramreddy

To cite this article: D. Srinivasacharya & C. Ramreddy (2013) Natural Convection Heat and Mass Transfer in a Micropolar Fluid with Thermal and Mass Stratification, International Journal for Computational Methods in Engineering Science and Mechanics, 14:5, 401-413, DOI: 10.1080/15502287.2013.784378

To link to this article: https://doi.org/10.1080/15502287.2013.784378

International Journal for Computational Methods in Engineering Science and Mechanics, 14:401–413, 2013

ISSN: 1550-2287 print / 1550-2295 online
DOI: 10.1080/15502287.2013.784378

Taylor & Francis
Taylor & Francis Group

Natural Convection Heat and Mass Transfer in a Micropolar Fluid with Thermal and Mass Stratification

D. Srinivasacharya and C. RamReddy
Department of Mathematics, National Institute of Technology, Warangal, Andhra Pradesh, India

The effects of thermal and solutal stratification on natural convection along a vertical plate embedded in a micropolar fluid are analyzed in both cases of buoyancy-assisting and buoyancy-opposing flows. The nonlinear governing equations and their associated boundary conditions are initially cast into dimensionless forms by pseudo-similarity variables. The resulting system of equations is then solved numerically using the Keller-box method. The numerical results are compared and found to be in good agreement with previously published results as special cases of the present investigation. The velocity, microrotation, temperature, and concentration profiles are shown for different values of the coupling number, thermal, and solutal stratification parameters. The numerical values of the skin friction, wall couple stress, heat and mass transfer rates for different values of governing parameters are also tabulated.

Keywords Natural convection, Micropolar fluid, Thermal stratification, Solutal stratification

1. INTRODUCTION

Natural convection flow is caused by buoyancy forces which arise from density differences in a fluid. These density differences are consequence of temperature gradients within the fluid. Natural convection flows are of great interest because of their various engineering, scientific, and industrial applications in heat and mass transfer, which include the fields of design of chemical processing equipment, formation and dispersion of fog, distributions of temperature and moisture over agricultural fields and groves of fruit trees, and damage of crops due to freezing and pollution of the environment. Extensive studies of natural convection heat and mass transfer of a non-isothermal vertical surface under boundary layer approximation for Newtonian fluids have been undertaken by several authors. Somers [1] has obtained theoretical results for combined thermal and mass transfer from a flat plate. Mather et al. [2] have considered the simultaneous heat and mass transfer in free convection. Theoretical solution of simultaneous heat and mass transfer by free convection about a vertical flat plate has been obtained by Bottemanne [3]. The interaction between heat and mass transfer in natural convection along a isothermal vertical surface has been studied by Schenk et al. [4]. Chen and Yuh [5] have considered the combined heat and mass transfer in natural convection along a vertical cylinder. A detailed review of free convective heat and mass transfer can be found in the book by Bejan [6].

In many problems of practical interest, natural convection flows arise in a thermally stratified environment. The input of thermal energy in enclosed fluid regions, a clue to the discharge of hot fluid or heat removal from heated bodies, often leads to the generation of a stable thermal stratification. Stratification of fluid arises due to temperature variations, concentration differences, or the presence of different fluids. Previous studies (for a comprehensive review, see Gebhart et al. [7]) have shown that stratification increases the local heat transfer coefficient and decreases the velocity and buoyancy levels. Another considerable effect of the stratification on the mean field is the formation of a region with a temperature deficit (i.e., a negative dimensionless temperature) and flow reversal in the outer part of the boundary layer. This phenomenon was first shown theoretically by Prandtl [8] for an infinite wall and later on by Jaluria and Himasekhar [9] for semi-infinite walls. Murthy et al. [10] and Lakshmi Narayana and Murthy [11] reported that the temperature and concentration became negative in the boundary layer depending on the relative intensity of the thermal and solutal stratification.

Only a few experimental studies were carried out on vertical free convection in a stratified environment. Jaluria and Gebhart [12] studied the stability of the flow adjacent to a vertical plate dissipating a uniform heat flux into a stratified medium both theoretically and experimentally. For this case, a theoretical similarity solution exists in which the ambient stratification varies like $x^{1/5}$, where x is the downstream coordinate. Unlike the case of linear stratification, the flow reversal and temperature deficit in this case [12], where the variation of the ambient temperature is relatively weak, are extremely small. A

Address correspondence to D. Srinivasacharya, Department of Mathematics, National Institute of Technology, Warangal, 506004, India. E-mail: dsrinivasacharya@yahoo.com

mathematical model is presented for the two-dimensional, steady, incompressible, laminar-free convection flow boundary layer flow over a continuously moving plate immersed in a thermally stratified, high-porosity, non-Darcian porous medium by Beg et al. [13]. Cheng [14] considered the combined heat and mass transfer in natural convection flow from a vertical wavy surface in a power-law fluid saturated porous medium with thermal and mass stratification. More recently, Srinivasacharya et al. [15] analyzed the effects of magnetic field and double dispersion on free convection heat and mass transfer along a vertical plate embedded in a doubly stratified non-Darcy porous medium saturated with power-law fluid.

The effects of heat and mass transfer in non-Newtonian fluid have great significance in engineering applications, such as the thermal design of industrial equipment dealing with molten plastics, polymeric liquids, foodstuffs, or slurries. The micropolar fluid model introduced by Eringen [16] exhibits some microscopic effects arising from the local structure and micromotion of the fluid elements. Further, they can sustain couple stresses. Micropolar fluids have been shown to accurately simulate the flow characteristics of polymeric additives, geomorphological sediments, colloidal suspensions, hematological suspensions, liquid crystals, lubricants, etc. The main advantage of using a micropolar fluid model compared to other non-Newtonian fluids is that it takes care of the rotation of fluid particles by means of an independent kinematic vector called the microrotation vector. The mathematical theory of equations of micropolar fluids and applications of these fluids in the theory of lubrication and porous media is presented by Lukaszewicz [17]. The heat and mass transfer in micropolar fluids is also important in the context of chemical engineering, aerospace engineering, and also industrial manufacturing processes. The problem of free convection heat and mass transfer in the boundary layer flow along a vertical surface submerged in a micropolar fluid has been studied by a number of investigators. The boundary layer flow of a micropolar fluid over a semi-infinite plate has been studied by Ahmadi [18]. Takhar and Soundalgekar [19] have considered the heat transfer on a semi-infinite plate of micropolar fluid. Rees and Pop [20] have examined theoretically the steady free convection from a vertical isothermal flat plate immersed in a micropolar fluid. EL-Hakiem et al. [21] studied natural convection with combined thermal and mass diffusion boundary effects in micropolar fluids. Cheng [22] has considered the fully developed natural convection heat and mass transfer of a micropolar fluid in a vertical channel with asymmetric wall temperatures and concentrations. Cheng [23] examined the natural convection heat and mass transfer near a sphere with constant wall temperature and concentration in a micropolar fluid. A coordinate transformation is used to transform the governing equations into non-dimensional, non-similar boundary layer equations and the resultant boundary layer equations are then solved by the cubic spline collocation method. Chang and Lee [24] analyzed flow and heat transfer characteristics of the free convection on a vertical plate with uniform and constant heat flux in a thermally stratified micropolar fluid. Srinivasacharya and RamReddy [25] studied the mixed convection heat and mass transfer along a vertical plate embedded in a micropolar fluid saturated non-Darcy porous medium by taking into account the thermal and solutal stratification effects.

The aim of the present paper is to study the free convection heat and mass transfer along a vertical plate with uniform wall temperature and concentration embedded in a stable, micropolar fluid with thermal and mass stratification. The Keller-box method given in the work by Cebeci and Bradshaw [26] is employed to solve the nonlinear system of this particular problem. The effects of micropolar, thermal, and mass stratification parameters are examined and are displayed through graphs. The results are compared with relevant results in the existing literature and are found to be in good agreement.

2. MATHEMATICAL FORMULATION

Consider the steady free convection heat and mass transfer along a vertical plate of length L embedded in a stable, a doubly stratified micropolar fluid. Choose the coordinate system such that x-axis is along the vertical plate and y-axis normal to the plate. The physical model and coordinate system are shown in Fig. 1. The plate is maintained at uniform wall temperature and concentration T_w, and C_w respectively. The ambient medium is assumed to be vertically linearly stratified with respect to both temperature and concentration in the form $T_\infty(x) = T_{\infty,0} + Ax$ and $C_\infty(x) = C_{\infty,0} + Bx$, respectively, where A and B are constants and varied to alter the intensity of stratification in the medium. The values of T_w and C_w are assumed to be greater than the ambient temperature $T_{\infty,0}$ and concentration $C_{\infty,0}$ at any arbitrary reference point in the medium (inside the boundary layer).

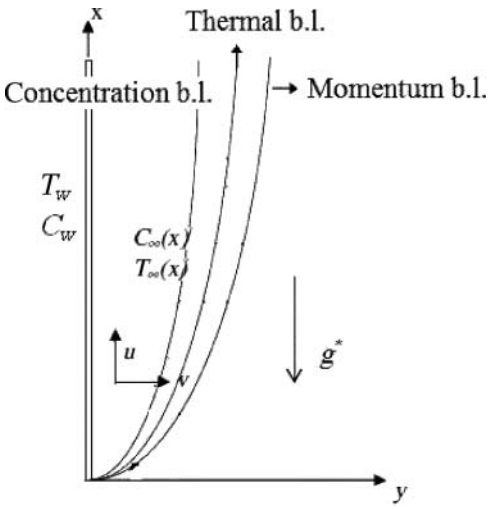

FIG. 1. Physical model and coordinate system.

Using the Boussinesq and boundary layer approximations, the governing equations for the micropolar fluid are given by

$$\frac{\partial u}{\partial x}+\frac{\partial v}{\partial y}=0 \tag{1}$$

$$\rho\left(u\frac{\partial u}{\partial x}+v\frac{\partial u}{\partial y}\right)=(\mu+\kappa)\frac{\partial^2 u}{\partial y^2}+\kappa\frac{\partial \omega}{\partial y}+\rho g^*(\beta_T(T-T_\infty)+\beta_C(C-C_\infty)) \tag{2}$$

$$\rho j\left(u\frac{\partial \omega}{\partial x}+v\frac{\partial \omega}{\partial y}\right)=\gamma\frac{\partial^2 \omega}{\partial y^2}-\kappa\left(2\omega+\frac{\partial u}{\partial y}\right) \tag{3}$$

$$u\frac{\partial T}{\partial x}+v\frac{\partial T}{\partial y}=\alpha\frac{\partial^2 T}{\partial y^2} \tag{4}$$

$$u\frac{\partial C}{\partial x}+v\frac{\partial C}{\partial y}=D\frac{\partial^2 C}{\partial y^2} \tag{5}$$

where u and v are the velocity components in x and y directions, respectively, ω is the component of micro-rotation whose direction of rotation lies in the xy-plane, T is the temperature, C is the concentration, g^* is the acceleration due to gravity, ρ is the density, μ is the dynamic coefficient of viscosity, β_T is the coefficient of thermal expansion, β_C is the coefficient of solutal expansions, κ is the vortex viscosity, j is the micro-inertia density, γ is the spin-gradient viscosity, α is the thermal diffusivity, and D is the solutal diffusivity of the medium.

The boundary conditions are

$$u=0,\ \ v=0,\ \ \omega=-n\frac{\partial u}{\partial y},\ \ T=T_w,\ \ C=C_w \quad at \quad y=0 \tag{6a}$$

$$u=0,\ \ \omega=0,\ \ T=T_\infty(x),\ \ C=C_\infty(x) \quad as \quad y\to\infty \tag{6b}$$

where k is the thermal conductivity of the fluid, the subscripts w, $(\infty, 0)$ and ∞ indicate the conditions at the wall, at some reference point in the medium, and at the outer edge of the boundary layer, respectively, and n is a constant such that $0 \le n \le 1$. Generally, when $n = 0$, Equation (6a) yields $\omega(x, 0) = 0$. This represents the case of concentrated particle flows in which the microelements close to the wall are not able to rotate. The case corresponding to $n = 0.5$ results in the vanishing of antisymmetric part of stress tensor and represents weak concentrations. The particle spin is equal to fluid vorticity at the boundary for the fine particle suspensions. The case corresponding to $n = 1$ is representative of turbulent boundary layer flows ([18, 27]). Thus for $n = 0$, particles are not free to rotate near the surface, whereas, as n increases from 0 to 1, the microrotation term gets augmented and induces flow enhancement.

In view of the continuity equation (1), we introduce the stream function ψ by

$$u=\frac{\partial \psi}{\partial y},\quad v=-\frac{\partial \psi}{\partial x} \tag{7}$$

Substituting (7) in (2)-(5) and then using the following pseudo-similarity transformations

$$\left.\begin{aligned}&\xi=\frac{x}{L},\quad \eta=\frac{Gr^{1/4}}{L\xi^{1/4}}y,\quad \psi=\frac{\mu Gr^{1/4}\xi^{3/4}}{\rho}f(\xi,\eta),\\ &\omega=\frac{\mu Gr^{3/4}\xi^{1/4}}{\rho L^2}g(\xi,\eta),\quad \theta(\xi,\eta)=\frac{T-T_{\infty,0}}{T_w-T_{\infty,0}}\\ &-\frac{Ax}{T_w-T_{\infty,0}},\quad \phi(\xi,\eta)=\frac{C-C_{\infty,0}}{C_w-C_{\infty,0}}-\frac{Bx}{C_w-C_{\infty,0}}\end{aligned}\right\} \tag{8}$$

we get the following nonlinear system of differential equations.

$$\left(\frac{1}{1-N}\right)f'''+\frac{3}{4}ff''-\frac{1}{2}(f')^2+\left(\frac{N}{1-N}\right)g'+\theta+\mathcal{B}\phi=\xi\left[f'\frac{\partial f'}{\partial \xi}-f''\frac{\partial f}{\partial \xi}\right] \tag{9}$$

$$\lambda g''+\frac{3}{4}fg'-\frac{1}{4}f'g-\left(\frac{N}{1-N}\right)\mathcal{J}\xi^{1/2}(2g+f'')=\xi\left[f'\frac{\partial g}{\partial \xi}-g'\frac{\partial f}{\partial \xi}\right] \tag{10}$$

$$\frac{1}{Pr}\theta''+\frac{3}{4}f\theta'-\varepsilon_1\xi f'=\xi\left[f'\frac{\partial \theta}{\partial \xi}-\theta'\frac{\partial f}{\partial \xi}\right] \tag{11}$$

$$\frac{1}{Sc}\phi''+\frac{3}{4}f\phi'-\varepsilon_2\xi f'=\xi\left[f'\frac{\partial \phi}{\partial \xi}-\phi'\frac{\partial f}{\partial \xi}\right] \tag{12}$$

where the primes indicate partial differentiation with respect to η alone, $Gr=\frac{g^*\beta_T(T_w-T_{\infty,0})L^3}{\nu^2}$ is the thermal Grashof number, $Pr=\frac{\nu}{\alpha}$ is the Prandtl number, $Sc=\frac{\nu}{D}$ is the Schmidt number, $\mathcal{J}=\frac{L^2}{jGr^{1/2}}$ is the micro-inertia density, $\lambda=\frac{\gamma}{j\rho\nu}$ is the spin-gradient viscosity, and $N=\frac{\kappa}{\mu+\kappa}$ $(0\le N<1)$ is the Coupling number [28]. We notice that for $N = 0$, where the flow, temperature, and concentration fields are unaffected by the microstructure of the fluid and the microrotation component is a passive quantity, the present problem reduces to that of a viscous fluid. $\mathcal{B}=\frac{\beta_C(C_w-C_{\infty,0})}{\beta_T(T_w-T_{\infty,0})}$ is the buoyancy ratio. When $\mathcal{B} = 0$, the flow is driven by thermal buoyancy alone. Further, the parameter $\mathcal{B} > 0$ represents the aiding buoyancy and $\mathcal{B} < 0$ represents the opposing buoyancy. $\varepsilon_1=\frac{AL}{T_w-T_{\infty,0}}$ and $\varepsilon_2=\frac{BL}{C_w-C_{\infty,0}}$ are the thermal and solutal stratification parameters.

Boundary conditions (6) in terms of f, g, θ and ϕ become

$$\begin{aligned}\eta &= 0:\ f'(\xi,0)=0,\ f(\xi,0)=\frac{-4}{3}\xi\left(\frac{\partial f}{\partial \xi}\right)_{\eta=0},\\ g(\xi,0) &= -n.f''(\xi,0)\\ \theta(\xi,0) &= 1-\varepsilon_1\xi,\ \phi(\xi,0)=1-\varepsilon_2\xi \qquad (13a)\\ \eta &\to \infty:\ f'(\xi,\infty)=0,\ G(\xi,\infty)=\theta(\xi,\infty)\\ &= \phi(\xi,\infty)=0 \qquad (13b)\end{aligned}$$

If $\varepsilon_1 = 0$ and $\varepsilon_2 = 0$, the problem reduces to free convection heat and mass transfer on a vertical plate with uniform wall temperature and concentration in an unstratified micropolar fluid,

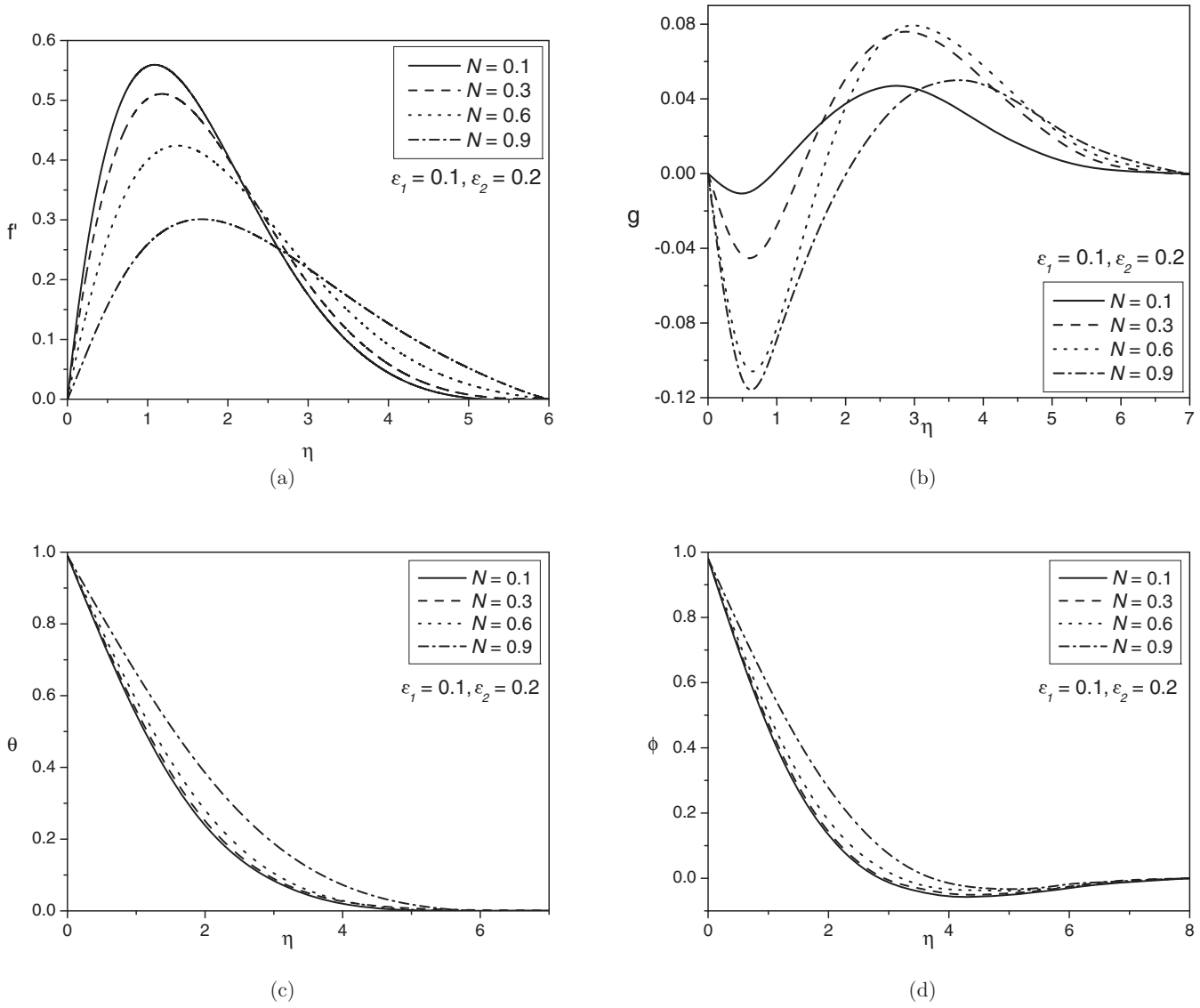

FIG. 2. (a) Velocity; (b) microrotation; (c) temperature; and (d) concentration profiles for various values of N with $\mathcal{B} = 1.0$.

and for the stratification we have $\varepsilon_1 > 0$ and $\varepsilon_2 \neq 0$. In the limit, as $\mathcal{B} \to 0$, the governing equations (1)-(5) reduce to the corresponding equations for a free convection heat transfer in a micropolar fluids. Hence, the case of the coupling of wall conduction with laminar free convection heat transfer of an unstratified micropolar fluids along a isothermal vertical flat plate of Char and Cheng [29] can be obtained by taking $\varepsilon_1 = 0$, $\varepsilon_2 = 0$, $n = 0.5$, and $\mathcal{B} = 0$.

The wall shear stress and the wall couple stress are

$$\tau_w = \left[(\mu + \kappa)\frac{\partial u}{\partial y} + \kappa\omega\right]_{y=0}, \tag{14a}$$

$$m_w = \gamma\left[\frac{\partial \omega}{\partial y}\right]_{y=0} \tag{14b}$$

and the heat and mass transfers from the plate, respectively, are given by

$$q_w = -k\left[\frac{\partial T}{\partial y}\right]_{y=0} \tag{15a}$$

$$q_m = -D\left[\frac{\partial C}{\partial y}\right]_{y=0} \tag{15b}$$

The non-dimensional skin friction $C_f = \frac{2\tau_w}{\rho U_*^2}$, wall couple stress $M_w = \frac{m_w}{\rho U_*^2 L}$, the local Nusselt number $Nu_x = \frac{q_w x}{k(T_w - T_{\infty,0})}$ and local Sherwood number $Sh_x = \frac{q_m x}{D(C_w - C_{\infty,0})}$, where U_* is the

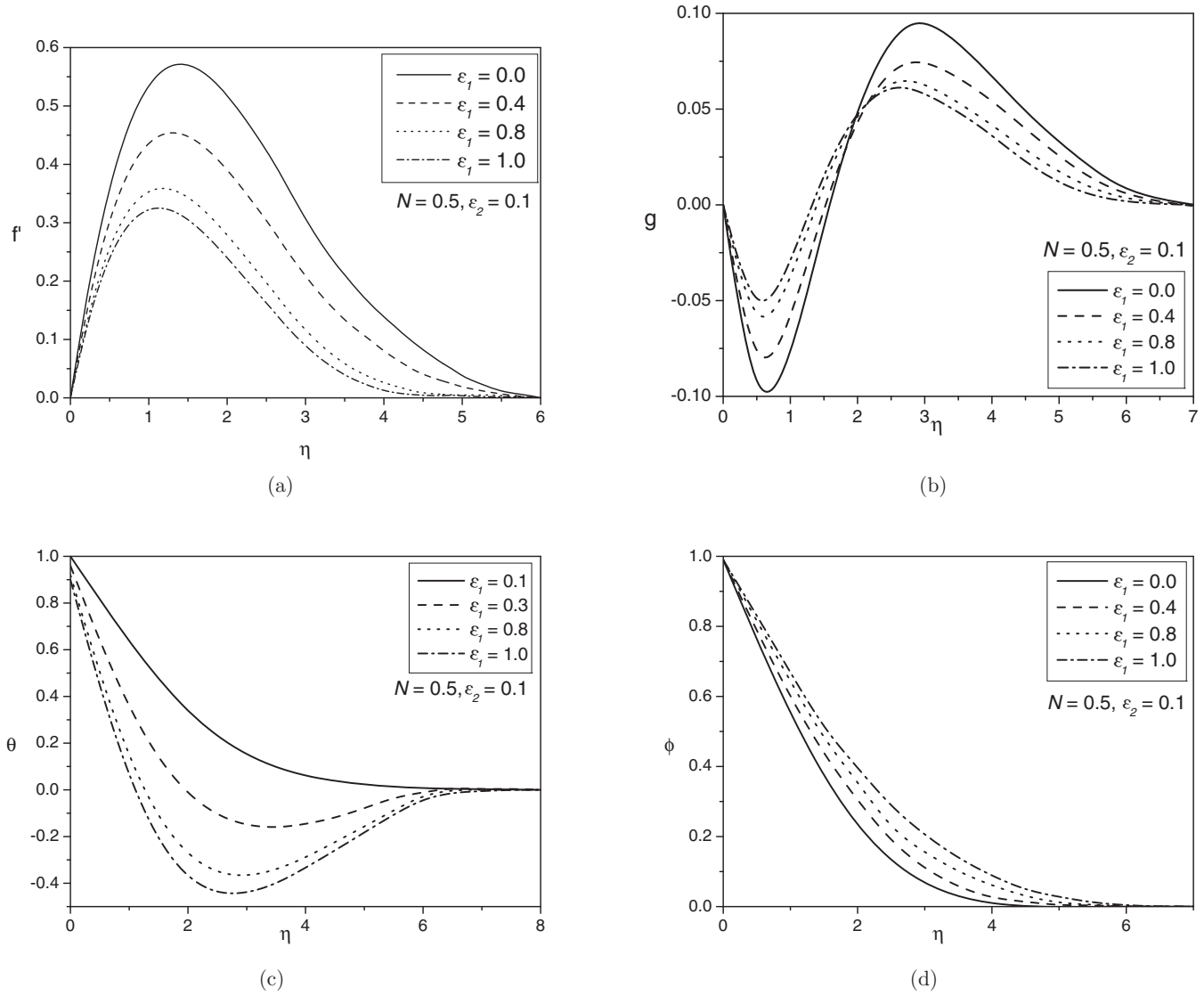

FIG. 3. (a) Velocity; (b) microrotation; (c) temperature; and (d) concentration profiles for various values of ε_1 with $\mathcal{B} = 1.0$.

characteristic velocity, are given by

$$C_f = 2\left(\frac{1-nN}{1-N}\right) Gr_x^{-1/4} f''(\xi, 0), \tag{16a}$$

$$M_w = \left(\frac{\lambda}{\mathcal{J}}\right) \xi^{1/2} Gr_x^{-1/2} g'(\xi, 0) \tag{16b}$$

$$Nu_x = -Gr_x^{1/4} \theta'(\xi, 0), \tag{16c}$$

$$Sh_x = -Gr_x^{1/4} \phi'(\xi, 0) \tag{16d}$$

where $Gr_x = \frac{g^* \beta_T (T_w - T_{\infty,0}) x^3}{\nu^2}$ is the local thermal Grashof number.

In terms of non-dimensional variables, the average Nusselt number and Sherwood numbers are

$$\frac{\overline{Nu}}{Gr_L^{1/4}} = \int_0^1 \xi^{-1/4} \theta'(\xi, 0) d\xi, \quad \frac{\overline{Sh}}{Gr_L^{1/4}} = \int_0^1 \xi^{-1/4} \phi'(\xi, 0) d\xi \tag{17}$$

3. RESULTS AND DISCUSSIONS

Flow Equations (9) and (10), which are coupled, together with the energy and concentration Equations (11) and (12), constitute nonlinear nonhomogeneous differential equations for which closed-form solutions cannot be obtained and hence we have to solve the problem numerically. Hence the governing boundary layer Equations (9) to (12) are solved numerically using the Keller-box implicit method discussed in the book by

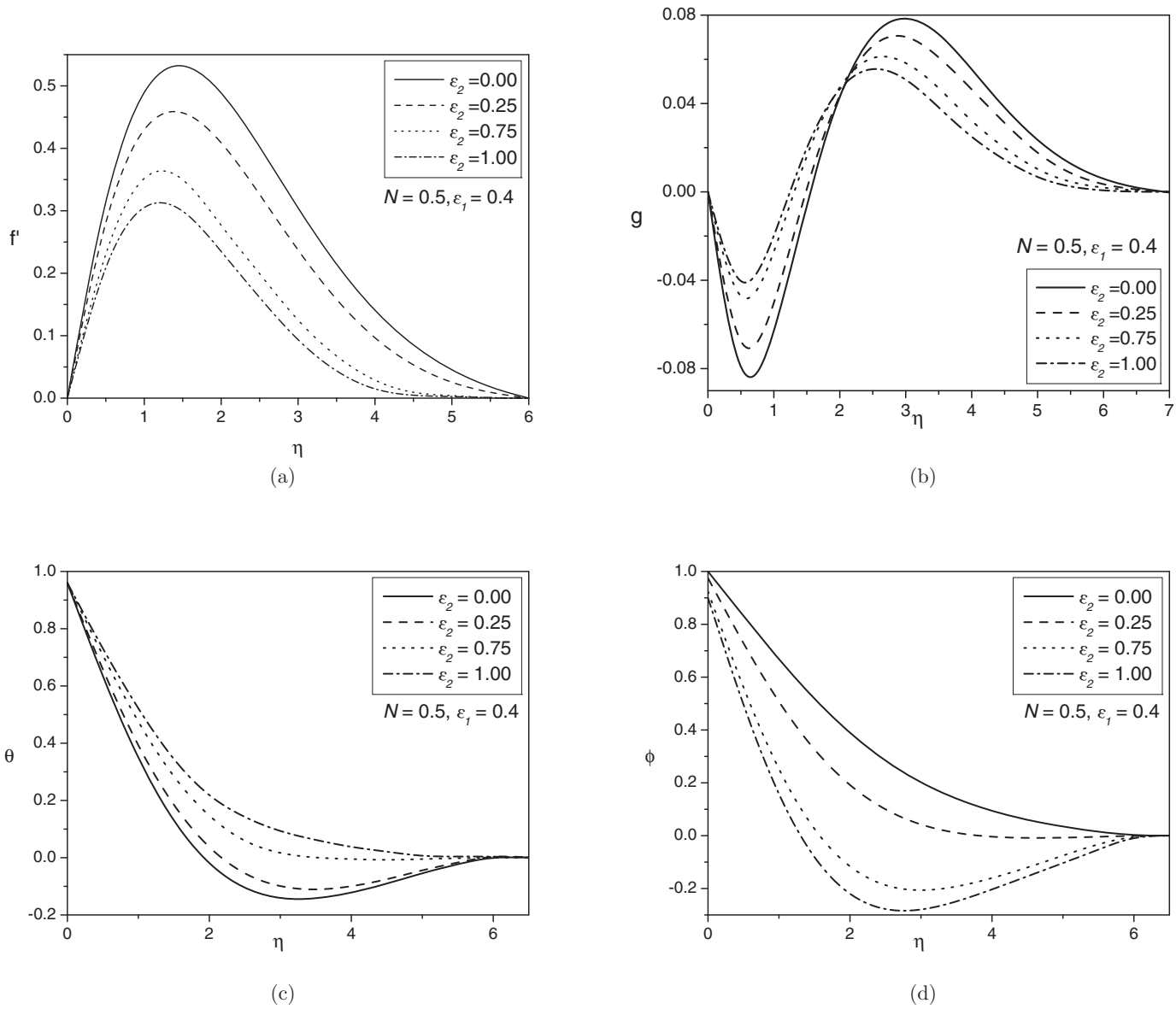

FIG. 4. (a) Velocity; (b) microrotation; (c) temperature; and (d) concentration profiles for various values of ε_2 with $\mathcal{B} = 1.0$.

Cebeci and Bradshaw [26]. This method has been proven to be adequate and gives accurate results for boundary layer equations. In the present study, the boundary conditions for η at ∞ are replaced by a sufficiently large value of η where the velocity, microrotation, temperature, and concentration profiles approach zero. We have taken $\eta_\infty = 7$ and a grid size of η of 0.01. We have computed the solutions for the dimensionless velocity, angular momentum, temperature and concentration function as shown graphically in Figures 2(a)–4(d). The effects of micropolar parameter N and stratification parameters ε_1 and ε_2 have been discussed in both cases of buoyancy-assisting and buoyancy-opposing flows. In order to reduce the number of parameters involved, computations were carried out for the cases of $Pr = 0.7$, $Sc = 0.7$, $n = 0$, and $\xi = 0.1$ while N, ε_1 and ε_2 were varied over a range. The values of $\mathcal{J} = 5.0$ and $\lambda = 5.0$ are chosen so as to satisfy the thermodynamic restrictions on the material parameters given by Eringen [16].

In the absence of buoyancy parameter $\mathcal{B}$, stratification parameters ε_1, and ε_2 with $N = 0.5$, $n = 0.5$, $\mathcal{J} = 50000$ and $\lambda = 5.0$, the results have been compared with the special case of laminar-free convection flow of micropolar fluids along an isothermal vertical flat plate [29] and it is found that they are in good agreement, as shown in Table 1.

The coupling number N characterizes the coupling of linear and rotational motion arising from the micromotion of the fluid molecules. Hence N signifies the coupling between the Newtonian and rotational viscosities. With a large value of N, the effect of microstructure becomes significant, whereas with

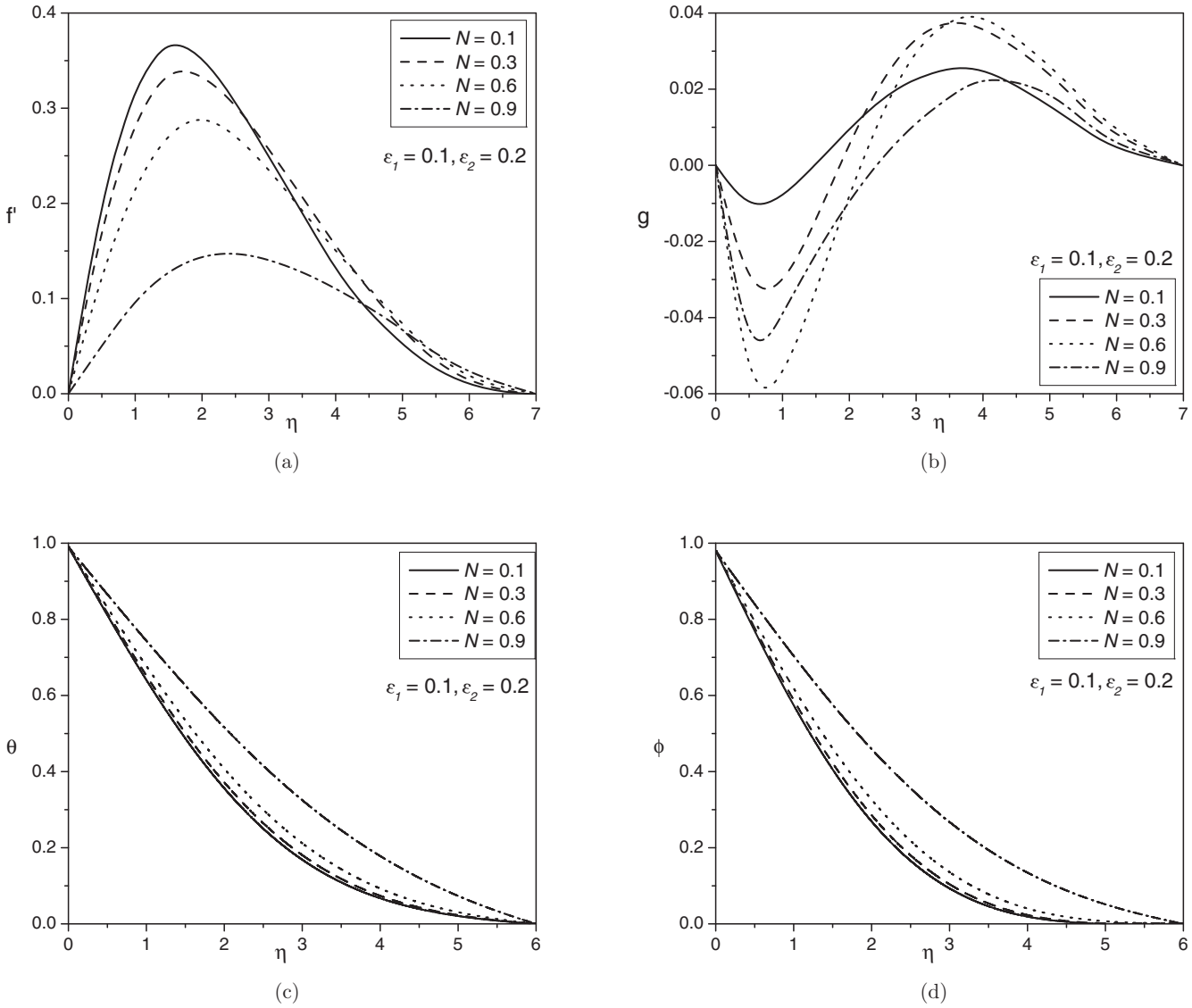

FIG. 5. (a) Velocity; (b) microrotation; (c) temperature; and (d) concentration profiles for various values of N with $\mathcal{B} = -0.5$.

a small value of N the individuality of the substructure is much less pronounced. As κ tend to zero, N also tends to zero, the micro-polarity is lost, and the fluid is to behave as non-polar fluid.

TABLE 1
Comparison of results for a vertical plate with unstratified case [29]

	$\overline{Nu}Gr^{-1/4}$	
Pr	Char and Cheng [29]	Present results
0.7	0.44600	0.44600
2.0	0.62809	0.62800
6.0	0.87825	0.87821
20.0	1.27226	1.27204

3.1 Aiding Buoyancy

In Figs. 2(a)–2(d), the effects of the coupling number N on the dimensionless velocity, microrotation, temperature, and concentration profiles are presented for fixed values of ε_1 and ε_2. As N increases, it can be observed from Fig. 2(a) that the maximum velocity decreases in amplitude and the location of the maximum velocity moves farther away from the wall. The velocity in the case of micropolar fluid is less compared to the case of the viscous fluid case ($N \to 0$ corresponds to viscous fluid). From Fig. 2(b), we observe that the microrotation changes sign from negative to positive values within the boundary layer. The microrotation tends to zero as $N \to 0$ as it is expected that in the limit $\kappa \to 0$, i.e., $N \to 0$, Eqs. (1) and (2) are uncoupled with (3) and they reduce to viscous fluid flow equations. From Fig. 2(c), we see that the temperature boundary layer thickness increases with the increase of coupling number N. It can be seen

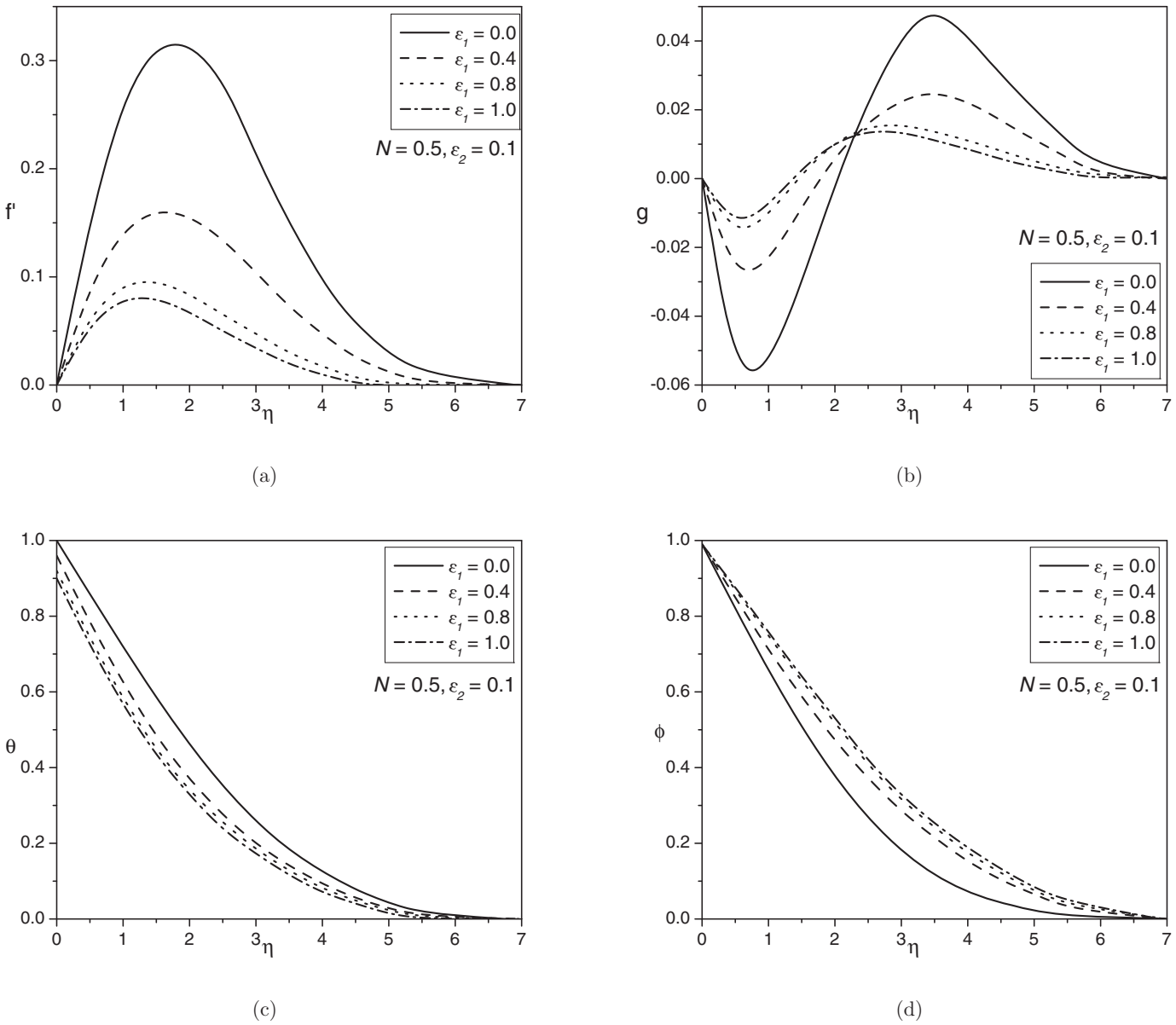

FIG. 6. (a) Velocity; (b) microrotation, (c) temperature; and (d) concentration profiles for various values of ε_1 with $\mathcal{B} = -0.5$.

from Fig. 2(d) that the concentration boundary layer thickness of the fluid increases with the increase of coupling number N. Furthermore, the temperature and concentration in case of micropolar fluids is more than that of the corresponding Newtonian fluid case.

Figure 3(a) displays the non-dimensional velocity for different values of thermal stratification parameter ε_1 for fixed values of N and ε_2. It is observed that the velocity of the fluid decreases with the increase of thermal stratification parameter. This is because thermal stratification reduces the effective convective potential between the heated plate and the ambient fluid in the medium. Hence, the thermal stratification effect reduces the velocity in the boundary layer. From Fig. 3(b), we observe that the microrotation changes sign from negative to positive values within the boundary layer. Also, it is clear that the magnitude of the microrotation increases with an increase in the thermal stratification parameter. The dimensionless temperature for different values of the thermal stratification parameter for $N = 0.5$ and $\varepsilon_2 = 0.1$ is shown in Fig. 3(c). It is clear that the temperature of the fluid decreases with the increase of the thermal stratification parameter. It is seen that the concentration of the fluid increases with the increase of the thermal stratification

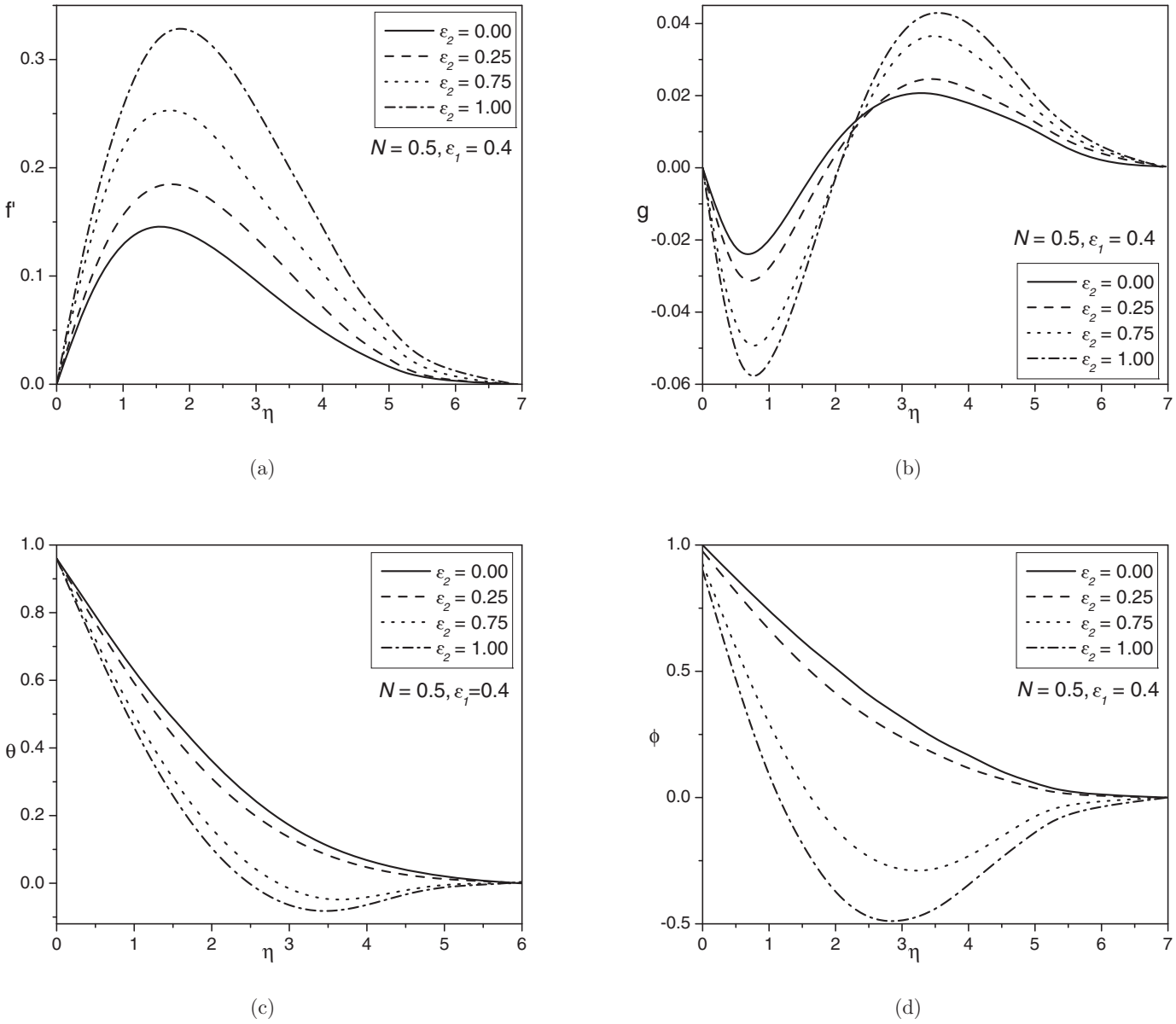

FIG. 7. (a) Velocity; (b) microrotation; (c) temperature; and (d) concentration profiles for various values of ε_2 with $\mathcal{B} = -0.5$.

parameter. When the thermal stratification effect is taken into consideration, the effective temperature difference between the plate and the ambient fluid will decrease; therefore, the thermal boundary layer is thickened and the temperature is reduced. Figure 3(d) demonstrates the dimensionless concentration for different values of thermal stratification parameter for $N = 0.5$ and $\varepsilon_2 = 0.1$. It can be noted that the effect of the stratification on the temperature is the formation of a region with a temperature deficit (i.e., a negative dimensionless temperature) in the case of micropolar fluid. This is in tune with the observation made in clear fluids and porous media. This phenomenon was reported in Refs. [7–11].

The dimensionless velocity component for different values of solutal stratification parameter ε_2 with constant N and ε_1 is depicted in Fig. 4(a). It is observed that the velocity of the fluid decreases with the increase of solutal stratification parameter. From Fig. 4(b), we notice that the microrotation changes sign from negative to positive within the boundary layer. Also, it is clear that the magnitude of the microrotation increases with an increase in solutal stratification parameter with $N = 0.5$ and $\varepsilon_1 = 0.4$. The dimensionless temperature for different values of solutal stratification parameter for $N = 0.5$ and $\varepsilon_1 = 0.4$ is displayed in Fig. 4(c). It is seen that the temperature of the fluid increases with the increase of solutal stratification

TABLE 2
Effect of skin friction and wall couple stress for various values of N, ε_1, and ε_2

			$\mathcal{B} = -0.5$		$\mathcal{B} = 1.0$	
N	ε_1	ε_2	$f''(\xi,0)$	$-g'(\xi,0)$	$f''(\xi,0)$	$-g'(\xi,0)$
0.0	0.1	0.2	0.55979	0.00000	1.48406	0.00000
0.1	0.1	0.2	0.52129	0.03644	1.38147	0.06450
0.3	0.1	0.2	0.43538	0.11842	1.15771	0.23864
0.5	0.1	0.2	0.33648	0.19431	0.90166	0.42849
0.7	0.1	0.2	0.22337	0.25243	0.60687	0.60612
0.9	0.1	0.2	0.08850	0.24790	0.25537	0.68093
0.5	0.0	0.1	0.35483	0.20750	0.96246	0.46802
0.5	0.2	0.1	0.28446	0.15609	0.90166	0.42849
0.5	0.4	0.1	0.22818	0.11350	0.84307	0.38936
0.5	0.6	0.1	0.19346	0.08805	0.78785	0.35153
0.5	0.8	0.1	0.17117	0.07323	0.73767	0.31656
0.5	1.0	0.1	0.15401	0.06269	0.69438	0.28655
0.5	0.4	0.00	0.21756	0.10549	0.87202	0.40884
0.5	0.4	0.25	0.24690	0.12773	0.80126	0.36080
0.5	0.4	0.50	0.28446	0.15609	0.73767	0.31656
0.5	0.4	0.75	0.32745	0.18777	0.68476	0.27999
0.5	0.4	1.00	0.37352	0.22077	0.64309	0.25229

parameter. Fig. 4(d) demonstrates the dimensionless concentration for different values of solutal stratification parameter with $N = 0.5$ and $\varepsilon_1 = 0.4$. It is clear that the concentration of the fluid decreases with the increase of thermal stratification parameter.

Table 2 shows the effects of the coupling number N on the skin friction parameter $f''(\xi,0)$ and the dimensionless wall couple stress $g'(\xi,0)$. It shows that the skin friction factor is lower for micropolar fluid than the Newtonian fluids ($N = 0$). Micropolar fluids offer a great resistance (resulting from vortex viscosity) to the fluid motion and cause larger skin friction factor compared to Newtonian fluid. The results also indicate that the large values of coupling number N lower wall couple stresses. The effects of the thermal stratification parameter ε_1 on the skin friction parameter $f''(\xi,0)$ and the dimensionless wall couple stress $g'(\xi,0)$ are presented in Table 2. It demonstrates that the skin friction parameter decreases while the wall couple stress increases as ε_1 increases. The results of Table 2 describe the effect of solutal stratification parameter ε_2 on the skin friction parameter $f''(\xi,0)$ and the dimensionless wall couple stress $g'(\xi,0)$. It is clear that the skin friction parameter decreases but the wall couple stress increases as ε_2 increases. Furthermore, the skin friction parameter is higher and wall couple stress parameter is lower for the unstratified fluid (i.e., $\varepsilon_1 = \varepsilon_2 = 0$) than for the stratified fluid (i.e., $\varepsilon_1 > 0$ and $\varepsilon_2 \neq 0$).

Table 3 displays the effect of coupling number N on the nondimensional heat and mass transfer coefficients with variation of the thermal stratification parameter ε_1 and solutal stratification parameter ε_2. It can be seen that the heat transfer coefficient increases with the increase of ε_1 for fixed values of N. Physically, positive values of the stratification parameter have the tendency to decrease the boundary layer thickness due to the reduction in the temperature difference between the plate and the free stream. This causes increases in the Nusselt number, as shown in Table 3. The decrease in the mass transfer coefficient causes with the increase of ε_1 for fixed values of N and ε_2 due to the effective mass transfer between the plate and the ambient medium decreases as the thermally stratified effect increases. The reverse trend can be observed in the case of ε_2. Also, for fixed values of both ε_1 and ε_2, the heat and mass transfer coefficients decrease with the increase of coupling number N. Further,

TABLE 3
Variation of non-dimensional heat and mass transfer rates versus ε_1 and ε_2 for different values of N with $\mathcal{B} = 1.0$

		$Nu_x Gr_x^{-1/4}$				$Sh_x Gr_x^{-1/4}$			
ε_1	ε_2	$N = 0.1$	$N = 0.3$	$N = 0.6$	$N = 0.9$	$N = 0.1$	$N = 0.3$	$N = 0.6$	$N = 0.9$
0.0	0.1	0.41281	0.39801	0.36485	0.28599	0.41625	0.40139	0.36793	0.28770
0.2	0.1	0.41706	0.40215	0.36854	0.28768	0.41366	0.39882	0.36551	0.28601
0.4	0.1	0.42109	0.40606	0.37200	0.28919	0.41105	0.39624	0.36307	0.28434
0.6	0.1	0.42492	0.40976	0.37524	0.29053	0.40841	0.39364	0.36061	0.28266
0.8	0.1	0.42853	0.41323	0.37825	0.29169	0.40575	0.39102	0.35815	0.28099
1.0	0.1	0.43191	0.41647	0.38103	0.29269	0.40308	0.38838	0.35567	0.27933
0.4	0.0	0.42248	0.40743	0.37330	0.29009	0.40898	0.39424	0.36128	0.28354
0.4	0.1	0.42109	0.40606	0.37200	0.28919	0.41105	0.39624	0.36307	0.28434
0.4	0.3	0.41832	0.40331	0.36939	0.28738	0.41501	0.40009	0.36646	0.28581
0.4	0.5	0.41551	0.40054	0.36676	0.28558	0.41877	0.40371	0.36963	0.28711
0.4	0.7	0.41269	0.39774	0.36412	0.28378	0.42230	0.40711	0.37258	0.28824
0.4	0.9	0.40984	0.39493	0.36147	0.28199	0.42561	0.41028	0.37529	0.28919
0.4	1.0	0.40841	0.39352	0.36014	0.28110	0.42718	0.41178	0.37656	0.28961

TABLE 4
Variation of non-dimensional heat and mass transfer rates versus ε_1 and ε_2 for different values of N with $\mathcal{B} = -0.5$

		$Nu_x Gr_x^{-1/4}$				$Sh_x Gr_x^{-1/4}$			
ε_1	ε_2	$N = 0.1$	$N = 0.3$	$N = 0.6$	$N = 0.9$	$N = 0.1$	$N = 0.3$	$N = 0.6$	$N = 0.9$
0.0	0.1	0.29716	0.28632	0.26254	0.21216	0.29877	0.28777	0.26355	0.21190
0.2	0.1	0.29459	0.28369	0.25981	0.20934	0.29310	0.28236	0.25892	0.20966
0.4	0.1	0.29144	0.28051	0.25663	0.20628	0.28735	0.27690	0.25430	0.20744
0.6	0.1	0.28770	0.27678	0.25298	0.20301	0.28154	0.27141	0.24969	0.20525
0.8	0.1	0.28338	0.27249	0.24888	0.19951	0.27567	0.26588	0.24510	0.20309
1.0	0.1	0.27847	0.26766	0.24434	0.19579	0.26976	0.26035	0.24054	0.20097
0.4	0.0	0.28990	0.27905	0.25538	0.20569	0.28457	0.27436	0.25240	0.20729
0.4	0.1	0.29144	0.28051	0.25663	0.20628	0.28735	0.27690	0.25430	0.20744
0.4	0.3	0.29451	0.28344	0.25911	0.20749	0.29309	0.28217	0.25828	0.20784
0.4	0.5	0.29756	0.28635	0.26160	0.20870	0.29905	0.28768	0.26249	0.20838
0.4	0.7	0.30059	0.28924	0.26409	0.20992	0.30524	0.29341	0.26694	0.20905
0.4	0.9	0.30360	0.29212	0.26658	0.21114	0.31165	0.29938	0.27162	0.20987
0.4	1.0	0.30509	0.29356	0.26782	0.21176	0.31493	0.30245	0.27405	0.21033

it can be noticed that the heat and mass transfer coefficients are more in the case of viscous fluids. This is because as N increases the thermal and solutal boundary layer thickness become large, thus giving rise to a small values of local heat and mass transfer rates. The skin friction coefficient as well as heat and mass transfer rates are lower in the micropolar fluid compared to the Newtonian fluid, which may be beneficial in flow, temperature, and concentration control of polymer processing. Therefore the presence of microscopic effects arising from the local structure and micromotion of the fluid elements reduce the heat and mass transfer rates.

3.2 Opposing Buoyancy

The influence of the parameter N on velocity, microrotation, temperature and concentration distributions, skin friction parameter, wall couple stress, and heat and mass transfer rates in the opposing buoyancy remains the same as in the case of aiding buoyancy, which shown in Figs. 5(a)–5(d) and in Table 2 and Table 4.

From Figs. 6(a)-6(d), we observe that the effect of the parameter ε_1 on velocity, microrotation, temperature, and concentration distributions in the opposing buoyancy is similar as in the case of aiding buoyancy. Also, the effect of ε_1 on the skin friction parameter and wall couple stress is found to be same as in the case of aiding buoyancy. Moreover, heat and mass transfer rates are decreasing with the increase of ε_1.

In Figs. 7(a)-7(d), the effect of ε_2 on velocity, microrotation, temperature, and concentration distributions in the case of opposing buoyancy is displayed. As ε_2 increases the velocity increases but temperature and concentration decrease. However, the effect of ε_2 on the skin friction parameter and the dimensionless wall couple stress in the opposing buoyancy is found to be opposite to the case of aiding buoyancy. Furthermore, heat and mass transfer rates are increasing with the increase of ε_2.

4. CONCLUSIONS

In this paper, we have presented a boundary layer analysis for free convection heat and mass transfer in a doubly stratified micropolar fluid over a vertical plate with uniform wall temperature and concentration conditions. Using the pseudo-similarity variables, the governing equations are transformed into a set of non-similar parabolic equations where a numerical solution has been presented for a wide range of parameters in both cases of buoyancy-assisting and buoyancy-opposing flows.

- The higher values of the coupling number N (i.e., for the case where the effect of microstructure becomes significant) result in lower velocity and microrotation distributions but higher wall temperature and wall concentration distributions in the boundary layer compared to the Newtonian fluid case ($N = 0$). The numerical results indicate that the skin friction and wall couple stresses in micropolar fluids are less than those obtained with Newtonian fluids. Also, non-dimensional heat and mass transfer coefficients decrease with the increase of the coupling number in the case of buoyancy-assisting flow. Further, the influence of N on velocity, microrotation, temperature and concentration distributions, skin friction parameter, wall couple stress, and heat and mass transfer rates in the opposing buoyancy remain the same as in the case of aiding buoyancy.
- An increase in thermal stratification parameter, and a decrease in velocity, temperature distributions, skin friction parameter, and non-dimensional mass transfer coefficient are accompanied by an increase in

non-dimensional heat transfer coefficient, concentration distribution, and wall couple stress in boundary layer in the case of buoyancy-assisting flow. Furthermore, we observed similar behavior on the various profiles but the opposite behavior on heat transfer rate in the case of opposing buoyancy compared to the case of aiding buoyancy.

- An increase in solutal stratification parameter, and a reduction in velocity, concentration distributions, skin friction parameter, and non-dimensional heat transfer coefficient result in enhanced temperature distribution, non-dimensional mass transfer coefficient, and wall couple stress in the boundary layer in the case of buoyancy-assisting flow. We see that the opposite behavior on velocity, temperature and skin friction, and wall couple stress result in same nature on concentration in the case of opposing buoyancy compared to the aiding buoyancy.
- We observe that the microrotation changes the sign from negative to positive values within the boundary layer in the presence of stratification. The results also indicate that skin friction and wall couple stresses are reduced in the case of micropolar fluid, when compared with the case of Newtonian fluid, in both cases of buoyancy-assisting and buoyancy-opposing flows.

NOMENCLATURE

A	Slope of ambient temperature.
B	Slope of ambient concentration.
$\mathcal{B}$	Buoyancy ratio.
C	Concentration.
C_w	Wall concentration.
C_f	Skin friction coefficient.
$C_{\infty,0}$	Ambient concentration.
D	Solutal diffusivity.
f	Reduced stream function.
g^*	Gravitational acceleration.
g	Dimensionless microrotation.
Gr	Thermal Grashof number.
Gr_x	Local thermal Grashof number.
j	Micro-inertia density.
$\mathcal{J}$	Dimensionless micro-inertia density.
k	Thermal conductivity.
L	Length of the plate.
M_w	Dimensionless wall couple stress.
m_w	Wall couple stress.
$\overline{Nu}$	Average Nusselt number.
Nu_x	Local Nusselt number.
N	Coupling number.
Pr	Prandtl number.
Sc	Schmidt number.
$\overline{Sh}$	Average Sherwood number.
Sh_x	Local Sherwood number.
T	Temperature.
T_w	Wall temperature.
$T_{\infty,0}$	Ambient temperature.
U_*	Characteristic velocity.
u, v	Velocity components in x and y directions.
x, y	Coordinates along and normal to the plate.
α	Thermal diffusivity.
β_T, β_C	Coefficients of thermal and solutal expansion.
γ	Spin-gradient viscosity.
η	Pseudo-similarity variable.
θ	Dimensionless temperature.
ϕ	Dimensionless concentration.
κ	Vortex viscosity.
λ	Dimensionless spin-gradient viscosity.
μ	Dynamic viscosity.
ν	Kinematic viscosity.
ξ	Dimensionless streamwise coordinate.
ρ	Density of the fluid.
τ_w	Wall shear stress.
ψ	Stream function.
ω	Component of microrotation .
ε_1, ε_2	Thermal and solutal stratification parameters.

SUBSCRIPTS

w	Wall condition.
∞	Ambient condition.
C	Concentration
T	Temperature

SUPERSCRIPT

$'$	Differentiation with respect to η.

REFERENCES

1. E.V. Somers, Theoretical Considerations of Combined Thermal and Mass Transfer from a Flat Plate, ASME J. Appl. Mech., vol. 23, pp. 295–301, 1956.
2. W.G. Mather, A.J. Madden, and E.L. Piret, Simultaneous Heat and Mass Transfer in Free Convection, Ind. Eng. Chem., vol. 49, pp. 961–968, 1957.
3. F.A. Bottemanne, Theoretical Solution of Simultaneous Heat and Mass Transfer by Free Convection about a Vertical Flat Plate, Appl. Sci. Res., vol. 25, pp. 137–149, 1971.
4. J. Schenk, R. Altmann, and J.P.A. Dewit, Interaction between Heat and Mass Transfer Simultaneous Natural Convection about an Isothermal Vertical Flat Plate, Appl. Sci. Res., vol. 32, pp. 599–606, 1976.
5. T.S. Chen and C.F. Yuh, Combined Heat and Mass Transfer in Natural Convection Along a Vertical Cylinder, I. J. Heat Mass Transfer, vol. 23, pp. 451–461, 1980.
6. A. Bejan, Convection Heat Transfer, John Wiley, New York, 2004.
7. B. Gebhart, Y. Jaluria, R. Mahajan, and B. Sammakia, Buoyancy lnduced Flows and Transport, Hemisphere Publishing co., New York, 1988.
8. L. Prandtl, Essentials of Fluid Dynamics, Blackie, London, 1952.
9. Y. Jaluria and K. Himasekhar, Buoyancy Induced Two Dimensional Vertical Flows in a Thermally Stratified Environment, Computer and Fluids, vol. 11, pp. 39–49, 1983.

10. P.V.S.N. Murthy, D. Srinivasacharya, and P.V.S.S.S.R. Krishna, Effect of Double Stratification on Free Convection in Darcian Porous Medium, J. Heat Transfer, vol. 126, pp. 476–484, 2004.
11. P.A. Lakshmi Narayana and P.V.S.N. Murthy, Free Convective Heat and Mass Transfer in a Doubly Stratified Non-Darcy Porous Medium, Journal of Heat Transfer, vol. 128, pp. 1204–1212, 2006.
12. Y. Jaluria and B. Gebhart, Stability and Transition of Buoyancy Induced Flows in a Stratified Medium, Journal of Fluid Mechanics, vol. 66, pp. 593–612, 1974.
13. A.O. Beg, J. Zueco, and H.S. Takhar, Laminar Free Convection from a Continuously-moving Vertical Surface in Thermally-stratified Non-Darcian High-porosity Medium: Network Numerical Study, Int. Commun. in Heat and Mass Transfer, vol. 35, pp. 810–816, 2008.
14. C.Y. Cheng, Combined Heat and Mass Transfer in Natural Convection Flow from a Vertical Wavy Surface in a Power-law Fluid Saturated Porous Medium with Thermal and Mass Stratification, Int. Comm. Heat Mass Transfer, vol. 36, pp. 351–356, 2009.
15. D. Srinivasacharya, J. Pranitha, and Ch. RamReddy, Magnetic and Double Dispersion Effects on Free Convection in a Non-Darcy Porous Medium Saturated with Power-law Fluid, Int. J. for Computational Methods in Engineering Science and Mechanics (accepted).
16. A.C. Eringen, Theory of Micropolar Fluids, J. Math. and Mech., vol. 16, pp. 1–18, 1966.
17. G. Lukaszewicz, Micropolar Fluids: Theory and Applications, Birkhauser, Basel, 1999.
18. G. Ahmadi, Self-similar Solution of Incompressible Micropolar Boundary Layer Flow over a Semi-infinite Plate, Int. J. Eng. Sci., vol. 14, pp. 639–646, 1976.
19. H.S. Takhar and V.M. Soundalgekar, Heat Transfer on a Semi-infinite Plate of Micropolar Fluid, Rheol. Acta, vol. 19, pp. 525–526, 1980.
20. D. Rees and I. Pop, Free Convection Boundary-layer Flow of a Micropolar Fluid from a Vertical Flat Plate, IMA Journal of Applied Mathematics, vol. 61, pp. 179–197, 1998.
21. M. EL-Hakiem, S.M.M. EL-Kabeir, and R.S.R. Gorla, Natural Convection from Combined Thermal and Mass Buoyancy Effects in Micropolar Fluids, Int. J. Fluid Mechanics Research, vol. 27, pp. 1–20, 2000.
22. C.Y. Cheng, Fully Developed Natural Convection Heat and Mass Transfer of a Micropolar Fluid in a Vertical Channel with Asymmetric Wall Temperatures and Concentrations, Int. Commun. Heat Mass Transfer, vol. 33, pp. 627–635, 2006.
23. C.Y. Cheng, Natural Convection Heat and Mass Transfer from a Sphere in Micropolar Fluids with Constant Wall Temperature and Concentration, Int. Commun. Heat Mass Transfer, vol. 35, pp. 750–755, 2008.
24. C.L. Chang and Z.Y. Lee, Free Convection on a Vertical Plate with Uniform and Constant Heat Flux in a Thermally Stratified Micropolar Fluid, Mechanics Research Communications, vol. 35, pp. 421–427, 2008.
25. D. Srinivasacharya and C. RamReddy, Effect of Double Stratification on Mixed Convection in a Micropolar Fluid Saturated Non-Darcy Porous Medium, Int. Review of Chemical Engineering, vol. 3, pp. 222–232, 2011.
26. T. Cebeci and P. Bradshaw, Physical and Computational Aspects of Convective Heat Transfer, Springer-Verlag, New York, 1984.
27. R.S.R. Gorla and A. Ameri, Boundary Layer Flow of a Micropolar Fluid on a Continuous Moving Cylinder, Acta Mech., vol. 57, pp. 203–214, 1985.
28. S.C. Cowin, Polar Fluids, Physics of Fluids, vol. 11, pp. 1919–1927, 1968.
29. M.I. Char and C.L. Cheng, Effect of Wall Conduction on Natural Convection Flow of Micropolar Fluids along a Flat Plate, Int. J. Heat Mass Transfer, vol. 40, pp. 3641–3652, 1997.